2F

PNL-3343
UC-70

High-Temperature Vitrification of Hanford Residual-Liquid Waste In a Continuous Melter

S. M. Barnes

April 1980

Prepared for the U.S. Department of Energy
under Contract DE-AC06-76RLO 1830

Pacific Northwest Laboratory
Operated for the U.S. Department of Energy
by Battelle Memorial Institute

Battelle

PNL-3343

NOTICE

PACIFIC NORTHWEST LABORATORY
operated by
BATTELLE
for the
UNITED STATES DEPARTMENT OF ENERGY
Under Contract DE-AC06-76RLO 1830

Printed in the United States of America
Available from
National Technical Information Service
United States Department of Commerce
5285 Port Royal Road
Springfield, Virginia 22151

Price: Printed Copy $_____*; Microfiche $3.00

*Pages	NTIS Selling Price
001-025	$4.00
026-050	$4.50
051-075	$5.25
076-100	$6.00
101-125	$6.50
126-150	$7.25
151-175	$8.00
176-200	$9.00
201-225	$9.25
226-250	$9.50
251-275	$10.75
276-300	$11.00

PNL-3343
UC-70

HIGH-TEMPERATURE VITRIFICATION OF HANFORD RESIDUAL-LIQUID WASTE IN A CONTINUOUS MELTER

S. M. Barnes

April 1980

Prepared for the
U.S. Department of Energy
under Contract DE-AC06-76RLO 1830

Pacific Northwest Laboratory
Richland, Washington 99352

SUMMARY

Over 270 kg of high-temperature borosilicate glass have been produced in a series of three short-term tests in the High-Temperature Ceramic Melter vitrification system at PNL. The glass produced was formulated to vitrify simulated Hanford residual-liquid waste. The tests were designed to 1) demonstrate the feasibility of utilizing high-temperature, continuous-vitrification technology for the immobilization of the residual-liquid waste, 2) test the airlift draining technique utilized by the high-temperature melter, 3) compare glass produced in this process to residual-liquid glass produced under laboratory conditions, 4) investigate cesium volatility from the melter during waste processing, and 5) determine the maximum residual-liquid glass production rate in the high-temperature melter.

The three tests with the residual-liquid composition confirmed the viability of the continuous-melting vitrification technique for the immobilization of this waste. Although minor processing difficulties (e.g., the formation of fused aggregates of unreacted feed) were encountered in the earlier tests, slight modification of the vitrification system and proper feed preparation produced excellent results in the later tests.

The airlift draining technique was demonstrated in these tests and the glass produced from the melter was shown to be less porous than the laboratory-produced glass. The airlift also was shown to be capable of satisfactorily draining glass from the melter during periods of discharge heater failure.

The final glass produced from the second test was compared to a glass of the same composition produced under laboratory conditions. A number of glass characteristics were compared, including porosity, softening and transition temperatures, heat capacity, leaching rate, thermal conductivity, and electrical resistivity. The comparative tests found the glasses to be indistinguishable, as the small differences in the test results fell within the precision range of the characterization testing equipment.

The cesium volatility was examined in the final test. Two melter effluent scrubbing systems were utilized to determine the cesium volatilization rate during processing. This examination showed that 0.44 wt% of the cesium (assumed to be cesium oxide) was volatilized, which translates to a volatilization rate of 115 mg/cm^2-h.

During later stages of the final residual-liquid test, the cold cap of unreacted feed in the melting cavity was accumulating, indicating that the maximum glass production rate had been achieved. This processing rate was found to be 18 kg/h of glass, representing a melting flux of 160 kg/m^2-h for the residual-liquid feed.

CONTENTS

FIGURES

TABLES

INTRODUCTION

The high-level liquid nuclear waste generated at Hanford from the reprocessing of defense-reactor spent fuel is currently stored in underground tanks. The originally acidic waste has been neutralized by the addition of sodium hydroxide. The neutralization has precipitated a metal hydroxide sludge from the liquid in the storage tanks. In a continuing program, the supernate is passed through evaporation and crystallization equipment for volume reduction. This process produces a salt cake and a residual liquid, which are stored in separate tanks. For long-term storage, a separate solidification process will be required to reduce the migration potential of the residual liquid.

One of the most promising nuclear waste immobilization techniques makes use of the ceramic-lined, continuous glass melter developed at the Pacific Northwest Laboratory (PNL) for the Department of Energy (Buelt et al. 1979). In this process, the high-level waste (HLW) is combined with glass formers to produce a durable, vitreous waste form for nuclear waste isolation.

Recently, high-temperature glass compositions[(a)] have been developed that exhibit improved durability (Rusin et al. 1979). This report summarizes a series of short tests with a high-temperature borosilicate glass formulation developed at Rockwell Hanford Operations (Kupfer 1979). This glass is designed to vitrify the radionuclide concentrate resulting from the radionuclide removal processing of Hanford defense residual liquid (Schulz 1980). The tests were performed at PNL in the High-Temperature Ceramic Melter (HTCM) vitrification system shown in Figure 1, and were funded by the Department of Energy through Rockwell Hanford Operations and PNL's High-Level Waste Immobilization Program.

(a) At PNL, high-temperature waste glasses are defined as those glasses that exhibit viscosities above 100 poise at 1050°C.

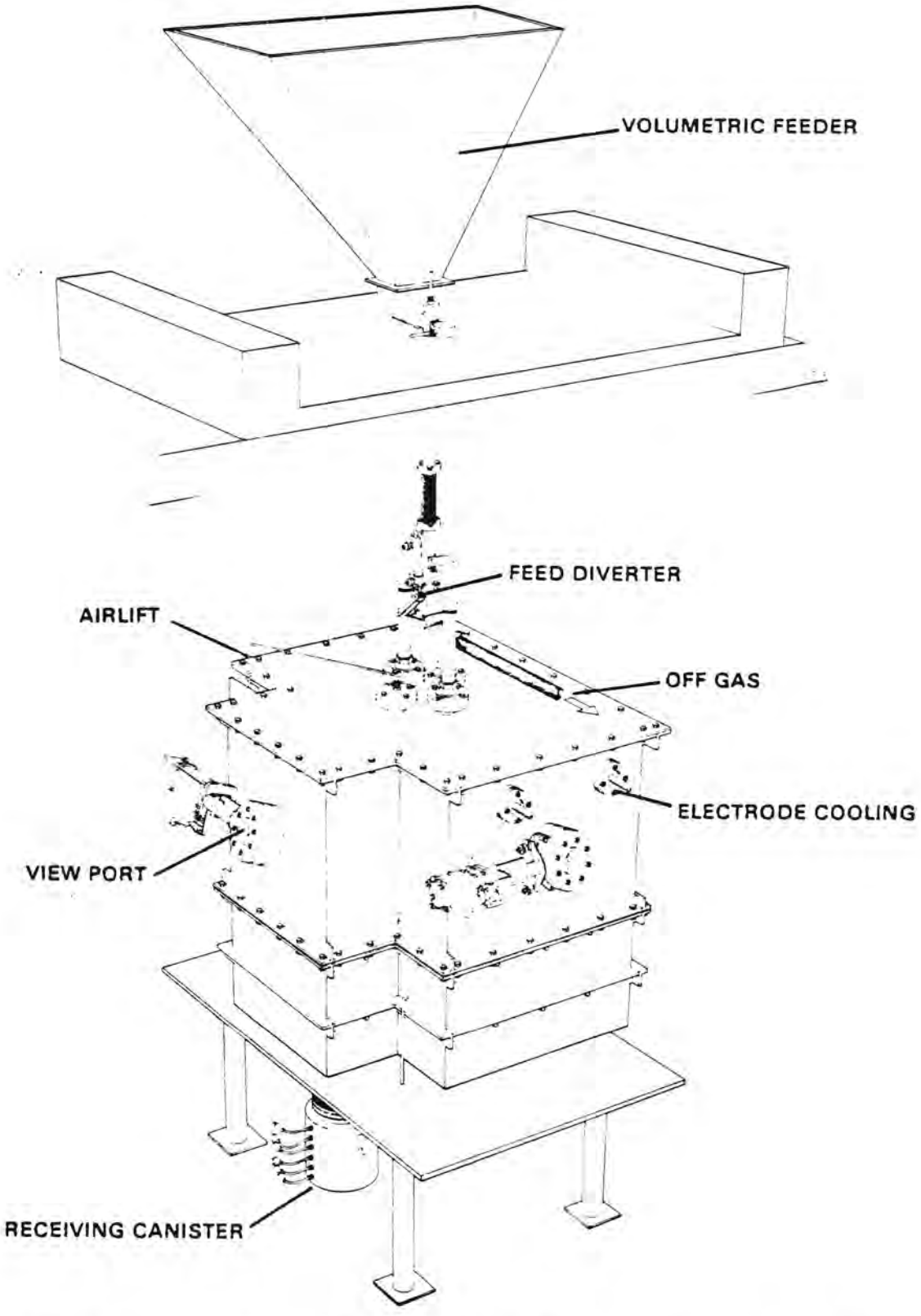

FIGURE 1. High-Temperature Ceramic Melter Vitrification System

PROCESS DESCRIPTION

The HTCM vitrification system is designed to convert simulated HLW to borosilicate glass and several other terminal waste storage forms. The HLW is simulated with dry chemicals that are mixed with glass-forming chemicals and fed continuously to the melter. The feed stream falls onto the molten glass surface and reacts to form the borosilicate waste glass. A portion of the glass product is periodically drained from the melter to a receiving canister using an airlifting technique. The vitrification system consists of three major components: the High-Temperature Melter, the Waste Feed System, and the Effluent Processing System.

HIGH-TEMPERATURE CERAMIC MELTER

The HTCM is a ceramic-lined, continuous electric glass melter designed to produce waste forms that may require processing temperatures approaching 1500°C. High-temperature operation has been achieved by building upon earlier PNL ceramic-melting technology with the incorporation of air-cooled tin oxide electrodes, highly insulative refractories, and a totally ceramic glass discharge system into the design. The HTCM dimensions are presented in Table 1. The HTCM is nominally operated in the range of 75 to 200 A, 70 to 200 V, 14 to 25 kW, and at less than 1500°C glass temperature.

To generate the heat required to maintain the molten glass, an alternating electric current is passed through the glass between the tin oxide electrodes.

TABLE 1. HTCM Dimensions

Dimension	Melting Cavity	Overall
Width	0.20 m	1.30 m
Length	0.61 m	1.37 m
Depth	0.63 m	1.42 m
Glass Depth	0.22 m	
Glass Volume = 26.7 ℓ	≃70 kg glass	

The power dissipated in the glass by this joule-heating effect is controlled by a constant electrode-current feedback system.

The HTCM primary drain shown in Figure 2 is designed to airlift the glass to the discharge trough. The glass flows through the trough and falls from the refractory pouring tip into the receiving canister. The canisters have a 31-cm ID, are 38 cm tall, and nominally contain 55 kg of glass. An alternative freeze-style drain is located at the center of the melting cavity floor to facilitate complete drainage of the melting cavity.

Simulated Waste Feed System

The premixed simulated waste and glass formers are delivered to the melter by a dual-screw volumetric feeder. The feed mixture is distributed over the long, narrow glass surface by a diverter valve, which alternates feed flow between twin feed addition ports. An air purge was added between the feeder and the diverter valve after the second residual-liquid glass test. This air purge is intended to reduce condensation of water vapor in the feed system from feed decomposition in the HTCM.

Effluent Processing System

Gaseous effluents generated by the decomposition of feed materials in the HTCM are processed by a scrubbing system prior to their release. The gases are first passed through a HEPA filter to remove entrained particulates, then through a venturi scrubber/condensor and a packed scrubbing column. The resulting filtered and scrubbed noncondensable gases are then exhausted to the building stack. The effluent system is shown schematically in Figure 3. The construction of the scrub-solution recycle system was not completed for the initial residual-liquid tests, so process water was used for once-through scrubbing. For the final residual-liquid tests, the recycle system and the offgas sampling system depicted in Figure 2 were used to obtain volatilization data.

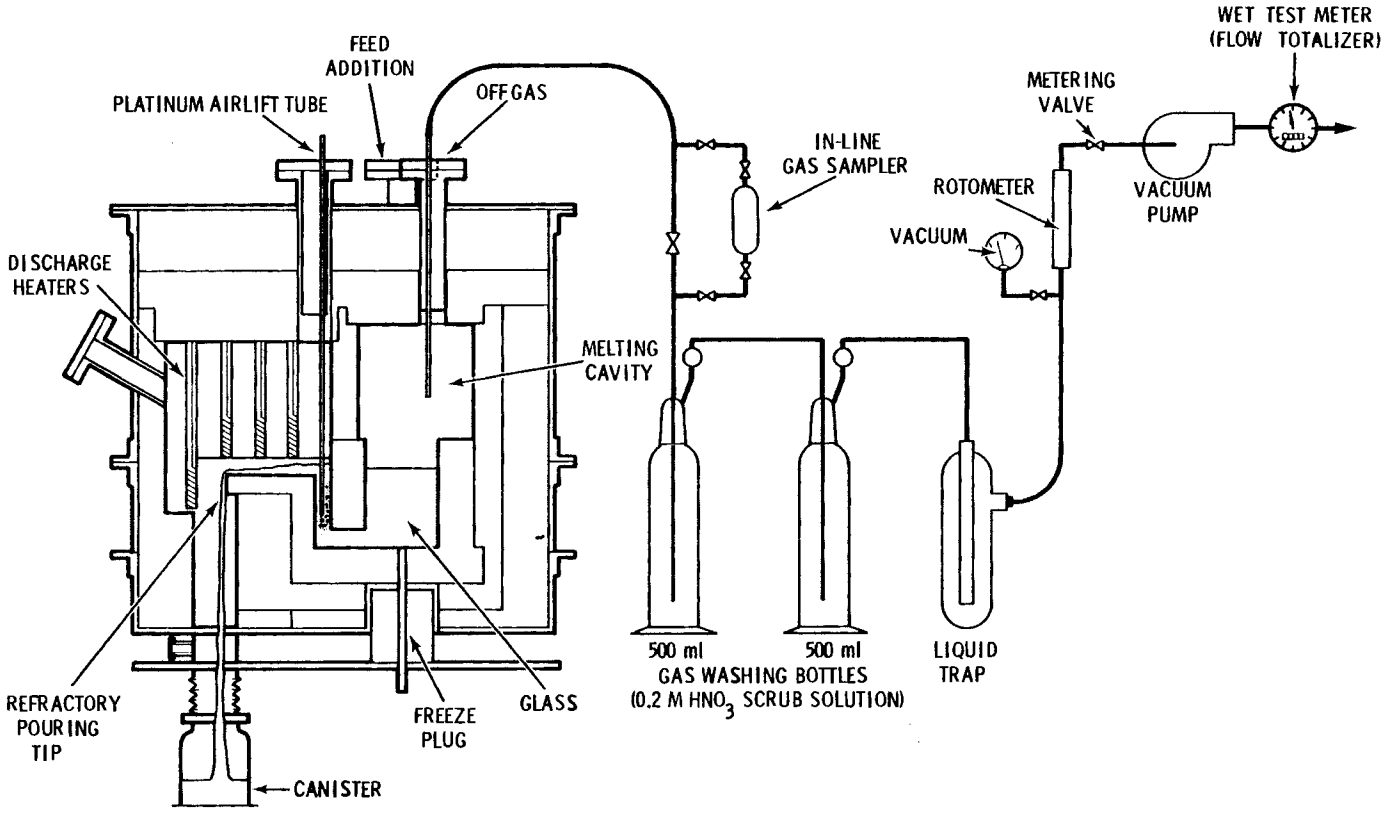

FIGURE 2. HTCM Primary Drain and Offgas Sampling System

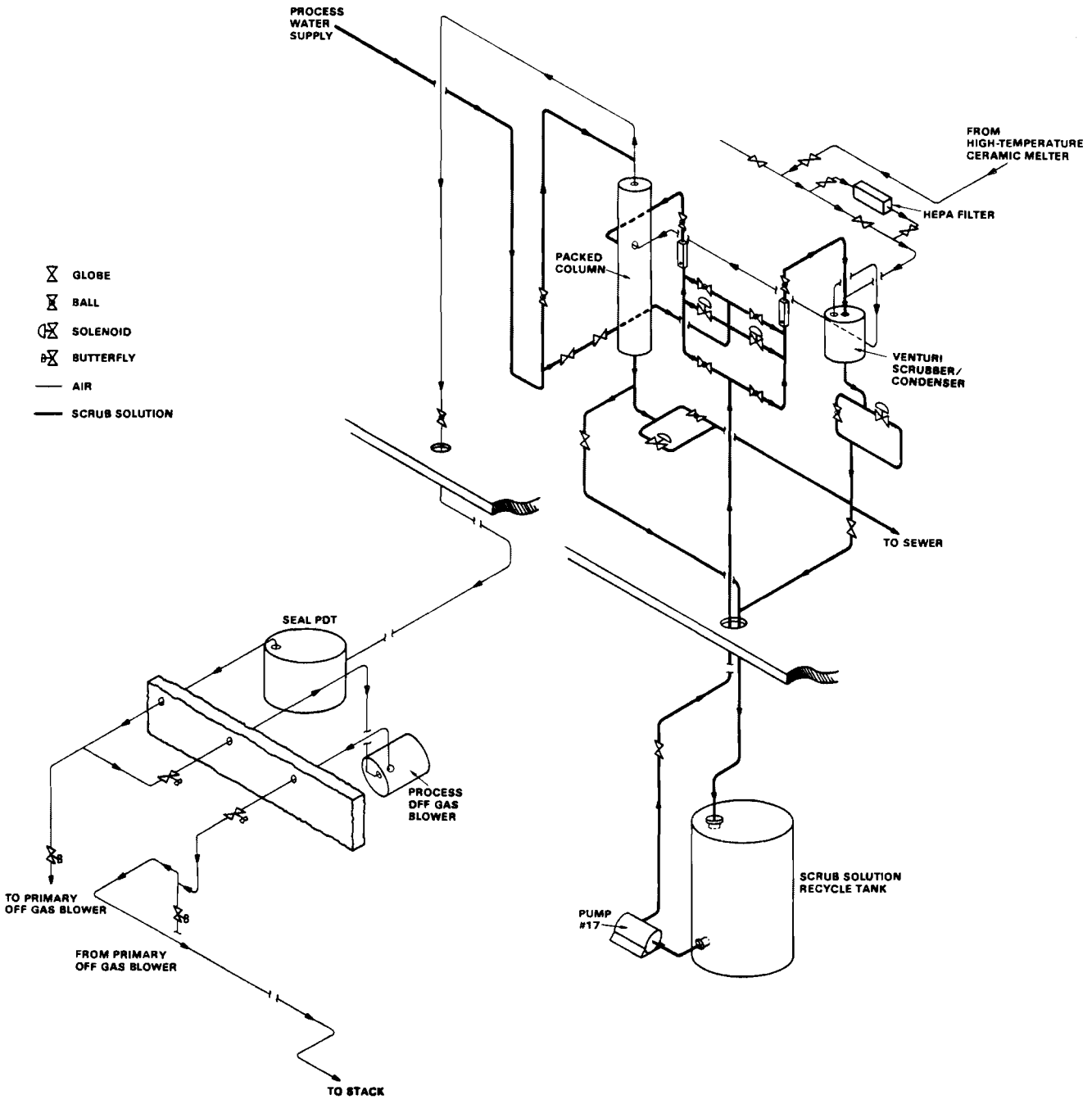

FIGURE 3. HTCM Effluent Processing System Schematic

EXPERIMENTAL

A series of three short-term tests (4- to 24-h durations) with the Hanford residual-liquid glass composition have been completed in the HTCM. The overall objective of these tests was to demonstrate the immobilization of simulated Hanford residual-liquid waste in high-temperature borosilicate glass. The following were established as objectives for the individual experiments.

TEST OBJECTIVES

Preliminary Tests, R-1

- observe glass composition processing characteristics
- test airlift draining technique
- optimize melter operation prior to test R-2;

Second Test, R-2

- demonstrate production of high-temperature waste glass
- compare high- and low-temperature glass processing
- obtain glass samples for comparison to laboratory-produced glass
- determine maximum glass production rate;

Third Test, R-3

- eliminate fused silica bodies
- investigate cesium volatility from the HTCM
- determine maximum glass production rate.

The composition of the Hanford residual-liquid waste, modified by the radionuclide removal process, is presented in Table 2. The table also lists waste glass formulation and the chemicals used in the feed preparation for the respective tests.

TEST RESULTS

Test R-1

The initial test demonstrated an average feedrate of 8.9 kg/h. Throughout this test, localized glass foam was observed on the molten surface surrounding

TABLE 2. Residual-Liquid Feed Compositions for Test R-1, R-2, and R-3

Compound	Residual-Liquid Waste, wt%	Resulting Waste Oxides, wt%	Glass Formers, wt%	Glass Composition, wt%	Added As R-1	Added As R-2	Added As R-3
SiO_2	---	---	78.8	63.0	SiO_2	SiO_2	SiO_2
B_2O_3	---	---	12.5	10.0	$Na_2B_4O_7$	$Na_2B_4O_7$	$Na_2B_4O_7$
Al_2O_3	---	4.1	6.2	5.9	$NaAlO_2$	$Al(OH)_3$	$NaAlO_2$ Al_2O_3
Li_2O	---	---	2.5	2.0	Li_2CO_3	Li_2CO_3	Li_2CO_3
Na_2O	---	86.5	---	17.3	Balance as Na_2CO_3	Balance as Na_2CO_3	Balance as Na_2CO_3
TiO_2	---	4.5	---	0.8	TiO_2	TiO_2	TiO_2
SrO	---	2.6	---	0.5	$SrCO_3$	$SrCO_3$	$Sr(NO_3)_2$
Cs_2O	---	2.2	---	0.4	Cs_2CO_3	$CsNO_3$	Cs_2CO_3
Na_2CO_3	67.5	---	---	---	---	---	---
$NaNO_3$	19.1	---	---	---	---	---	---
$NaAlO_2$	2.4	---	---	---	---	---	---
$NaTi_2O_5H$	3.9	---	---	---	---	---	---
NaOH	3.3	---	---	---	---	---	---
SrO	1.5	---	---	---	---	---	---
Cs_2CO_3	1.5	---	---	---	---	---	---

the reacting feed. The foam dissipated within a few centimeters of the feed and was attributed to an interaction between the residual-liquid glass and the other composition existing in the HTCM at the beginning of the test. Stable melter operation was achieved for several hours before a partial feed-system failure forced termination of the test. This failure resulted in overfeeding the melter, which produced extensive foaming throughout the entire melting cavity. A series of vertical glass temperature scans, Figure 4, were performed prior to the appearance of the foam (A), during the foaming period (B), and after the foam subsided (C). As in other continuous melters, the foam increased the glass temperature near the melter floor and decreased the glass temperature near the molten surface (McElroy 1980). These temperature changes are due to shifting of the normal electrical current paths because of the relatively high resistance of the foam layer.

After the foam receded, small (3- to 8-cm-dia) fused bodies of unreacted feed material were observed floating on the glass surface. A sample of the unreacted materials is pictured in Figure 5 and the chemical analysis is listed in Table 3.

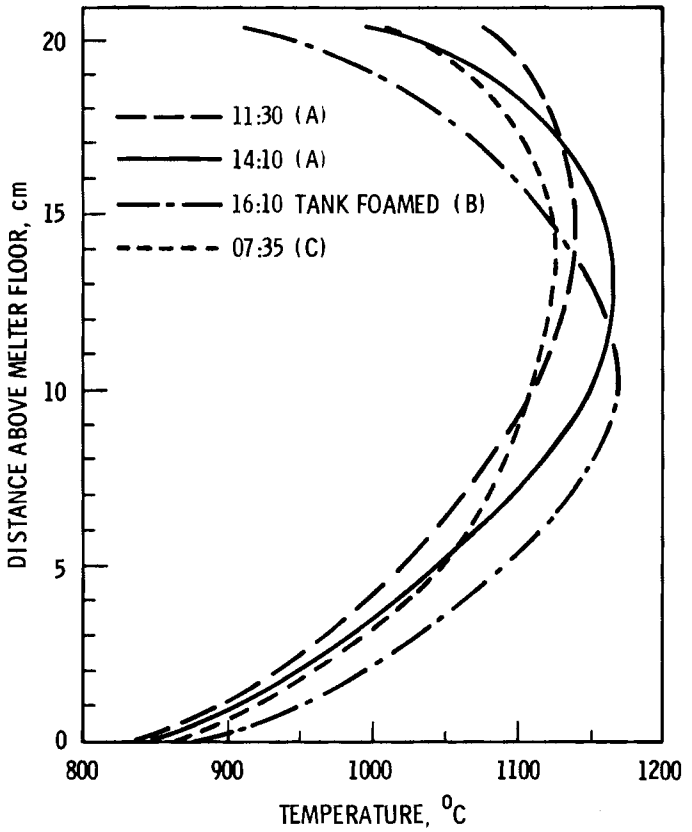

FIGURE 4. Vertical Temperature Profiles from Test R-1

The melter power consumption, glass temperature, and feed rates for this test are presented in Figure 6. The two power peaks correspond to periods when the insulating cold cap of unreacted feed was not present. The melter feedrate was not sufficient to maintain a cold cap in the first case, and the feed system shutdown at 1400 h allowed the cold cap to melt down in the second.

Test R-2

The fused silica bodies formed during R-1 had diminished in size, but were present at the onset of this test. Several steps were taken to inhibit the formation of additional fused bodies during R-2, including increasing the glass processing temperature and maintaining a low initial feedrate to eliminate the foaming.

As in the earlier test, slight foaming was observed near the unreacted feed. This foaming was markedly reduced as the glass composition in the

FIGURE 5. Fused Silica Bodies

TABLE 3. Chemical Analysis of Fused Silica Bodies and R-2 Feed Aggregates

Analysis Group	Al_2O_3	B_2O_3	Cs_2O	Fe_2O_3	Li_2O	Na_2O	SiO_2	SrO	TiO_2
Fused bodies from test R-1	1.72	2.74	0.25	0.11	0.98	4.79	85.3	0.38	0.77
Fused bodies from test R-2	2.68	2.98	0.21	0.11	0.87	6.54	81.6	0.42	0.85
Test R-2 feed aggregates	0.45	62.1	0.10	---	0.11	27.3	5.50	0.11	0.25

melter approached the residual-liquid formulation, confirming the glass interaction hypothesis. Seven hours into the test a stable, fully developed cold cap was present.

The development of the cold cap, however, created problems with the melter feed system. The water vapor created by the decomposition of the $Al(OH)_3$ began to condense in the relatively cool feedlines and the diverter valve. This condensation created blockages in feed system on numerous occasions, as noted in

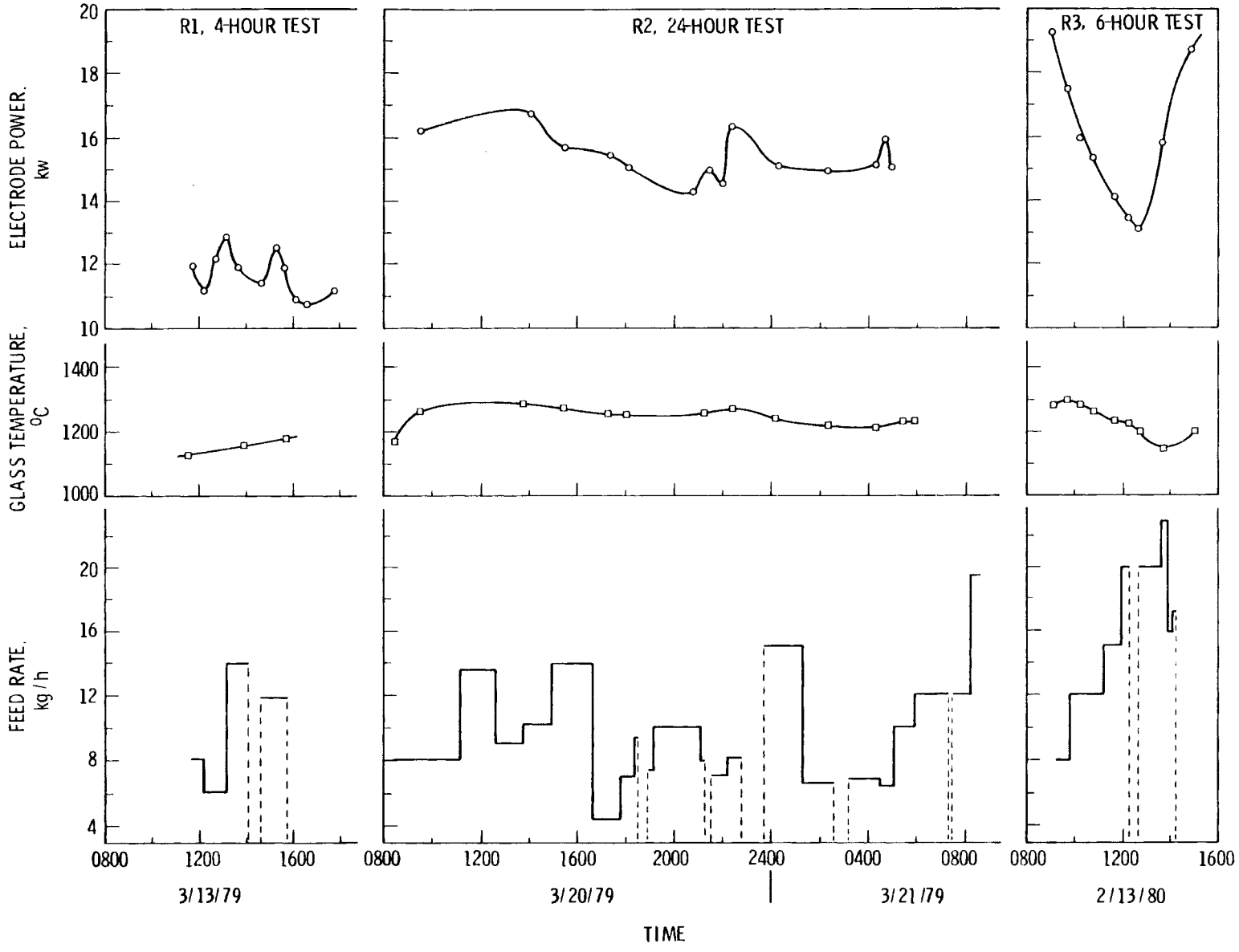

FIGURE 6. Residual-Liquid Testing Operating Data

the R-2 feedrate curve of Figure 6. The installation of the air purge in the feed system that followed this test has eliminated this problem.

Test R-2 demonstrated an average feedrate of 7.9 kg/h. The glass production was limited by the feed system, and the melter appeared capable of significantly increased feedrates. Another very positive aspect of the HTCM demonstrated by this test was the airlift draining technique. Early in the test the discharge heaters nearest to the refractory pouring tip failed. The airlift initiated and terminated the glass product flow rapidly enough to preclude many of the glass drainage problems associated with low discharge-region temperatures.

As before, the cold cap meltdown revealed the fused silica bodies. Another sample was taken and the chemical analysis is presented in Table 3. It was not possible to determine if the fused bodies were newly formed or remnants from R-1. Their presence did not noticeably impair the melter operation, and they dissolved within 75 h of the R-2 test termination. Subsequent examination of the R-2 feed revealed the presence of marble-sized clumps. Analysis of these aggregates presented in Table 3 showed them to be rich in boron and sodium. This indicated that the fused silica bodies were caused by feed segregation during preparation, and were not related to processing conditions in the melter.

A total of four canisters were filled during tests R-1 and R-2. The canisters were core-drilled to remove samples for analysis. The chemical composition of the core samples and the R-2 feed is listed in Table 4. The change in core sample density over the two tests is presented in Figure 7. Examination of Table 4 shows the product glass to be approaching the test R-2 feed oxide composition very well. The oxide weight percentage of the final glass core sample is within 10% of the R-2 feed analysis, and only 0.1 wt% impurities (BaO, CaO) remains in the samples from the initial glass composition existing in the melter prior to the residual-liquid testing. Also, plotted on the density figure are curves that predict the product glass density if the melting cavity is assumed to be exhibiting plug flow and perfectly mixed reactor characteristics. For both R-1 and R-2, the actual product density closely follows

TABLE 4. Chemical Composition of Core-Drilled Samples from R-2

Glass Throughput, kg	Glass Density, g/cm^3	Oxide, wt%														
		Al_2O_3	B_2O_3	BaO	CaO	Cr_2O_3	Cs_2O	Fe_2O_3	Li_2O	MnO_2	Na_2O	NiO	SiO_2	SrO	TiO_2	ZnO
10	2.646	6.58	12.7	0.78	1.22	0.37	0.06	3.01	2.48	0.45	12.7	0.52	46.0	1.18	2.37	0.62
20	2.643	6.71	13.0	0.79	1.24	0.38	0.06	3.03	2.68	0.47	13.6	0.54	47.6	1.22	2.45	0.62
30	2.645	6.33	12.7	0.76	1.19	0.35	0.06	2.94	2.53	0.45	13.0	0.51	46.6	1.19	2.41	0.58
36	2.624	5.90	11.8	0.59	0.87	0.39	0.17	2.33	2.18	0.30	13.7	0.36	49.3	0.91	1.77	0.48
54	2.592	5.47	11.3	0.50	0.72	0.29	0.18	1.64	2.17	0.25	13.8	0.29	52.4	0.83	1.62	0.40
68	2.597	5.70	11.8	0.50	0.76	0.31	0.20	1.63	2.54	0.25	14.6	0.31	55.1	0.83	0.55	0.41
82	2.593	5.49	11.3	0.46	0.68	0.29	0.21	1.53	2.20	0.23	14.3	0.28	53.8	0.83	1.60	0.37
96	2.544	5.35	11.0	0.30	0.44	0.19	0.26	0.95	2.21	0.14	15.8	0.17	58.7	0.68	1.30	0.25
110	2.537	5.02	10.4	0.15	0.23	0.12	0.30	0.39	2.14	0.08	16.2	0.06	60.0	0.55	1.04	0.12
124	2.530	5.05	10.1	0.13	0.23	0.08	0.31	0.26	2.16	0.02	16.2	0.05	62.2	0.54	1.01	0.11
138	2.522	5.19	10.3	0.08	0.11	0.06	0.30	0.15	2.47	---	17.8	0.02	65.4	0.55	0.99	0.07
157	2.517	4.73	9.6	0.05	0.08	0.04	0.33	0.13	1.99	---	14.7	---	61.0	0.55	0.95	0.04
175	2.516	4.64	10.2	0.05	0.07	---	0.24	0.12	2.01	---	15.8	---	62.3	0.51	0.90	0.04
194	2.522	4.52	10.7	0.05	0.06	---	0.34	0.11	1.92	---	15.9	---	62.2	0.51	0.88	---
207	2.516	4.54	10.9	0.03	0.07	---	0.31	0.09	2.02	---	16.1	---	62.4	0.51	0.88	---
R-2 Feed	---	4.45	9.9	---	---	---	0.33	0.05	1.97	---	16.1	---	66.5	0.51	0.97	---
"As-Defined" Residual-Liquid Glass	2.512	5.82	10.0	0.0	0.0	0.0	0.44	0.0	2.0	0.0	17.3	0.0	63.0	0.52	0.90	0.0

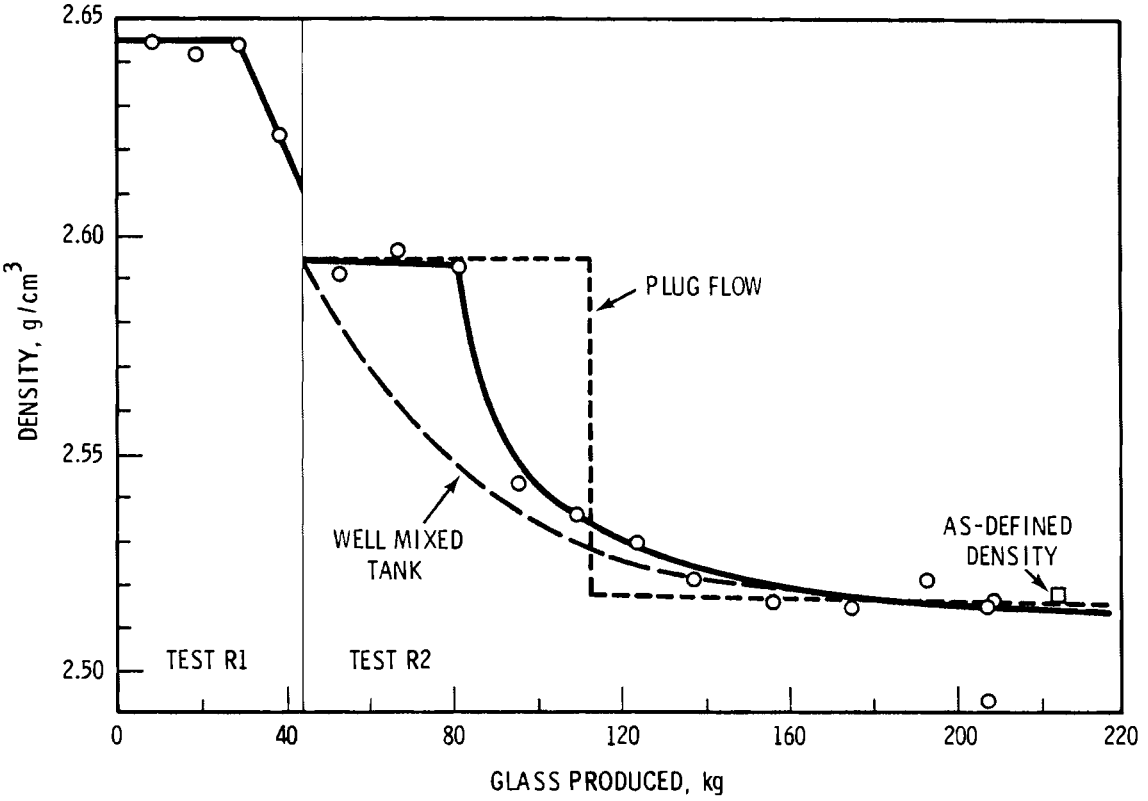

FIGURE 7. Density of Core-Drilled Samples Versus Total Glass Produced in Tests R-1 and R-2

the plug flow prediction for approximately 55 kg (about three quarters of the melter inventory), where the well mixed curve became the best predictor. This is the predicted result as the lower-density residual-liquid glass would tend to float on the more dense glass in the melter. This characteristic is also seen in the oxide weight percentage changes in Table 4 and is similar to the results reported by Chapman et al. (1979) for the depletion of zinc from the glass produced in another PNL melter.

The "as-defined" residual-liquid composition is also listed in Table 4. The discrepancies between the as-defined and the test R-2 feed have been traced to feed preparation errors, such as the substitution of $Al(OH)_3$ for the AlO(OH) originally intended.

Test R-3

The presence of the boron and sodium-rich aggregates in the R-2 feed prompted test R-3. This test was designed to confirm that proper feed preparation would preclude the fused silica body formation and to demonstrate increased glass production rates. In addition, the completion of the recirculating offgas scrub solution system provided the capability of measuring the cesium volatility from the residual-liquid composition.

The R-3 operational data is plotted in Figure 6. The steady decrease in electrode power and glass temperature is due to the reduced electrical resistivity of the residual-liquid composition relative to the glass present in the melter at the beginning of the test. Recalling that joule-power dissipation is defined as the product of the resistance and the square of the electrical current, any reduction in resistance would produce a corresponding power decrease in a constant-current system. When the glass temperature fell below 1200^{o}C, the electrode current, and thus the melter power, was increased manually as is shown in Figure 6. This resulted in the glass temperature increase desired.

Test R-3 demonstrated an average feedrate of 13.7 kg/h--an improvement of more than 50% over the earlier tests. This large increase was primarily due to the addition of the feed system air purge and the substitution of other aluminum compounds for the $Al(OH)_3$. This combination prevented water condensation in the feed system, resulting in significantly improved operation. Near the end of the test, the unreacted feed material cold cap appeared to be growing. This indicated that the maximum processing rate had been obtained for this composition in the HTCM ($\sim$20 kg/h). This feedrate translates to about 18 kg/h of glass production or a feed process flux of 160 kg/m^2-h, which compares favorably to experience with other PNL melters (Buelt et al. 1979). There were no fused bodies of unreacted feed present at the end of this test.

To investigate the residual-liquid effluents, data was gathered from the sampling system pictured in Figure 2 and the HTCM offgas system, Figure 3. The HEPA filter gained 147.5 g during test R-2. This gain represents 0.2% of the

feed added to the melter during R-2. A sample of the material collected on the HEPA filter was removed and analyzed. The results of this analysis are presented in Table 5. As was anticipated, the primary components of the HEPA sample were Al_2O_3, SiO_2, and TiO_2. The particle sizes of these oxides were the smallest of all chemicals used in the R-3 feed preparation, and therefore the most easily entrained in the offgases.

The scrub solutions were also analyzed for feed entrainment and volatiles. The results are presented in Table 5. The scrubbing systems were operated from feed initiation until the entire cold cap had reacted. Cesium was the major feed percentage-loss element. The combined HEPA and scrub solution losses constituted 0.44% of the cesium present in the feed. This loss corresponds to a volatilization rate of 115 mg/cm^2-h, or approximately half of the volatilization rate reported by W. J. Gray (1976) for a low-melting borosilicate waste glass at the 100-poise viscosity temperature (1050°C). The difference in volatilization is partially due to the presence of an unreacted-feed cold cap in the HTCM (Gray's experiments were conducted with bare molten glass surfaces), but other researchers report decreased cesium volatility with increased viscosity at constant temperature (Kupfer and Schulz 1973; Ross and Mendel 1980), indicating that cesium volatility is diffusion-limited. The comparable cesium volatilization rate at equal viscosities of the residual-liquid and low-temperature compositions is in agreement with these findings.

The analysis of the noncondensable gases collected from the HTCM offgas is compared to the composition of air in Table 5. The 50-fold increase in CO_2 is due to the decomposition of the carbonate feed chemicals. This increase in CO_2 is reflected in a 4% drop in the presence of O_2 and in the displacement of 3% of the atmospheric nitrogen.

Comparative Characterization of Residual-Liquid Glass

The final glass produced in test R-2 was compared to a laboratory-produced residual-liquid glass to confirm the quality of the continuous melter product. The glasses were analyzed for porosity, density, transition and softening temperatures, thermal expansion, specific heat, leach resistance, viscosity,

TABLE 5. Chemical Analysis of Test R-3 Effluents

Analysis Group	Al_2O_3	B_2O_3	Cs_2O	Li_2O	Na_2O	SiO_2	SrO	Ti_2O	Ar	CO	CO_2	N_2	O_2	Others
Collected on HEPA, g	2.4	1.3	0.4	2.0	3.5	133.1	0.5	2.4	---	---	---	---	---	---
Feed Loss on HEPA, %	0.2	<0.1	0.1	0.1	<0.1	0.3	0.1	0.4	---	---	---	---	---	---
Collected in Scrub Solution, g	0.3	5.6	1.0	1.1	2.7	9.4	0.5	<0.1	---	---	---	---	---	---
Feed Loss to Scrub Solution, %	<0.1	<0.1	0.2	<0.1	<0.1	<0.1	<0.1	<0.1	---	---	---	---	---	---
Total Feed Loss to Effluent System, %	0.2	<0.1	0.4	0.2	<0.1	0.3	0.2	0.4	---	---	---	---	---	---
Noncondensable Off-gases, mole%														
Collection Time														
1045	---	---	---	---	---	---	---	---	0.95	<0.10	3.45	74.5	21.1	<0.01
1405	---	---	---	---	---	---	---	---	0.93	<0.10	3.78	74.3	21.0	<0.01
1500	---	---	---	---	---	---	---	---	0.95	<0.10	2.97	74.8	21.3	<0.01

resistivity, and thermal conductivity. The results of these characterization tests are presented in Table 6 and Figures 8 through 10. Although the numerical values differ, the glasses are essentially indistinguishable because the small variation is within the error range of the characterization tests. The thermal conductivity test produced an especially large error range of ±10%. This is partially due to the translucent nature of the residual-liquid composition. The thermal diffusivity, from which the thermal conductivity is calculated, is measured by the time it takes for the heat produced by a laser pulse to travel from one surface of a small test specimen to the opposite surface. Because this glass is translucent, a graphite coating was applied to each of the surfaces of interest to prevent any of the laser energy from passing through the specimen as light. Any variation in the graphite thickness or coverage would influence the result and partially accounts for the data scatter observed.

TABLE 6. Comparative Characterization of the Residual-Liquid Glass

Characteristics	Produced in HTCM	Produced in Laboratory
Porosity	0.20%	0.21%
Density	2.52 g/cm^3	2.52 g/cm^3
Transition Temperature	504°C	504°C
Softening Temperature	546°C	535°C
Thermal Expansion (100 to 500°C)	2.64×10^{-5} cm/°C	2.54×10^{-5} cm/°C
Specific Heat at:		
100°C	0.20 cal/g-°C	0.20 cal/g-°C
200°C	0.23 cal/g-°C	0.23 cal/g-°C
300°C	0.25 cal/g-°C	0.25 cal/g-°C
400°C	0.25 cal/g-°C	0.26 cal/g-°C
450°C	0.26 cal/g-°C	0.26 cal/g-°C
Leaching Weight Loss		
Soxhlet (72-h, 99°C)	2.98×10^{-5} g/cm^2-d	4.11×10^{-5} g/cm^2-d
pH-4 (19-h, 23°C)	7.48×10^{-6} g/cm^2-d	5.99×10^{-6} g/cm^2-d
pH-9 (19-h, 23°C)	1.04×10^{-5} g/cm^2-d	3.16×10^{-6} g/cm^2-d

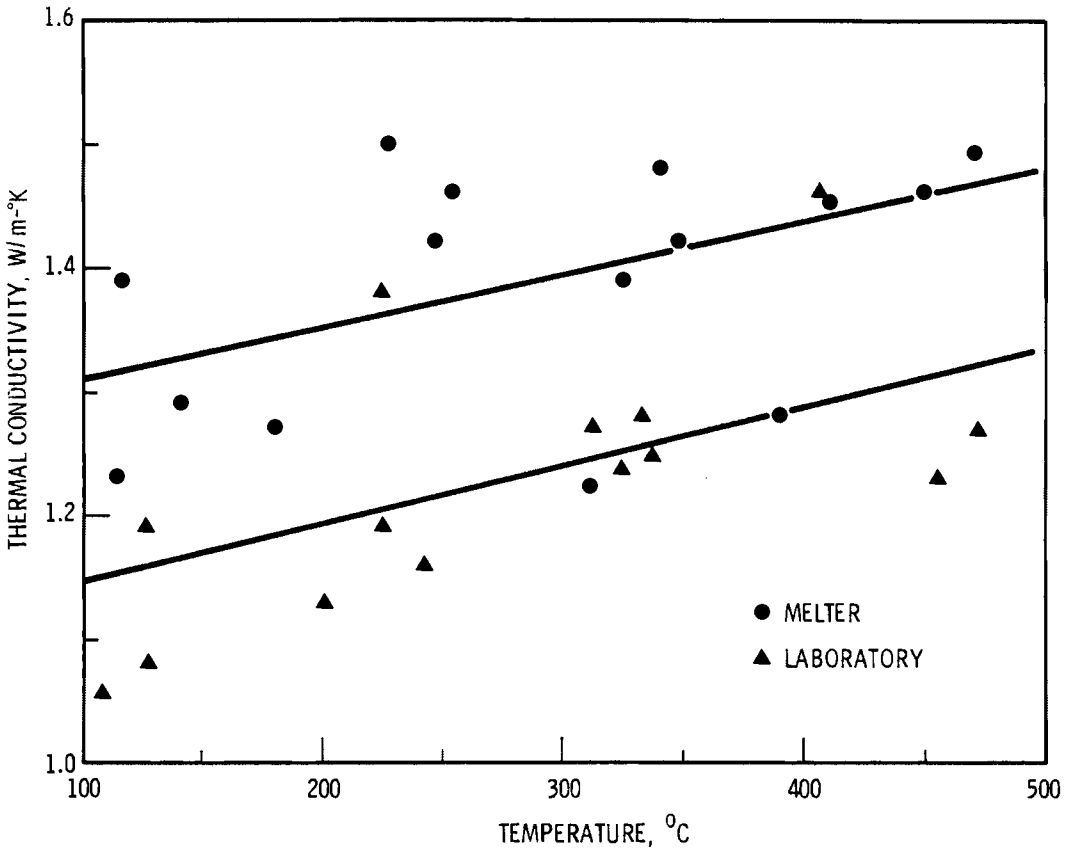

FIGURE 8. Thermal Conductivity Comparison of Melter- and Laboratory-Produced Glasses

One of the most significant results of this comparison is the nearly identical porosity of the laboratory- and melter-produced glasses. A major concern with the airlift draining technique had been the possible increase in product porosity due to the required air injection. This porosity increase was not observed, confirming the applicability of the airlift draining technique to continuous melting technology.

The leaching weight-loss percentage for this composition is compared to several standard, low-temperature glasses in Table 7. The residual-liquid glass is shown to be a durable waste host, as leach-testing results compare very favorably to the other waste glasses.

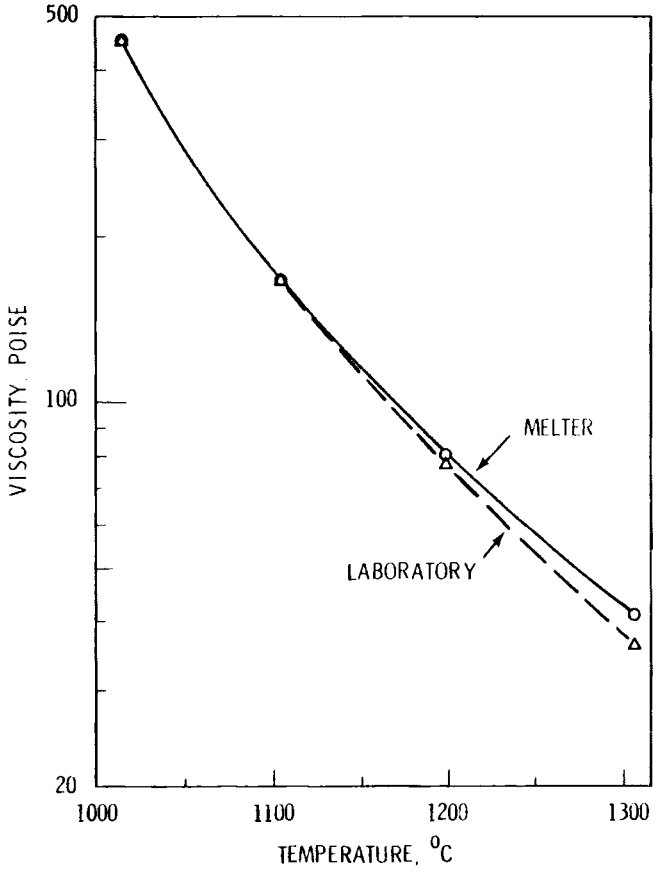

FIGURE 9. Viscosity Comparison of Melter- and Laboratory-Produced Glasses

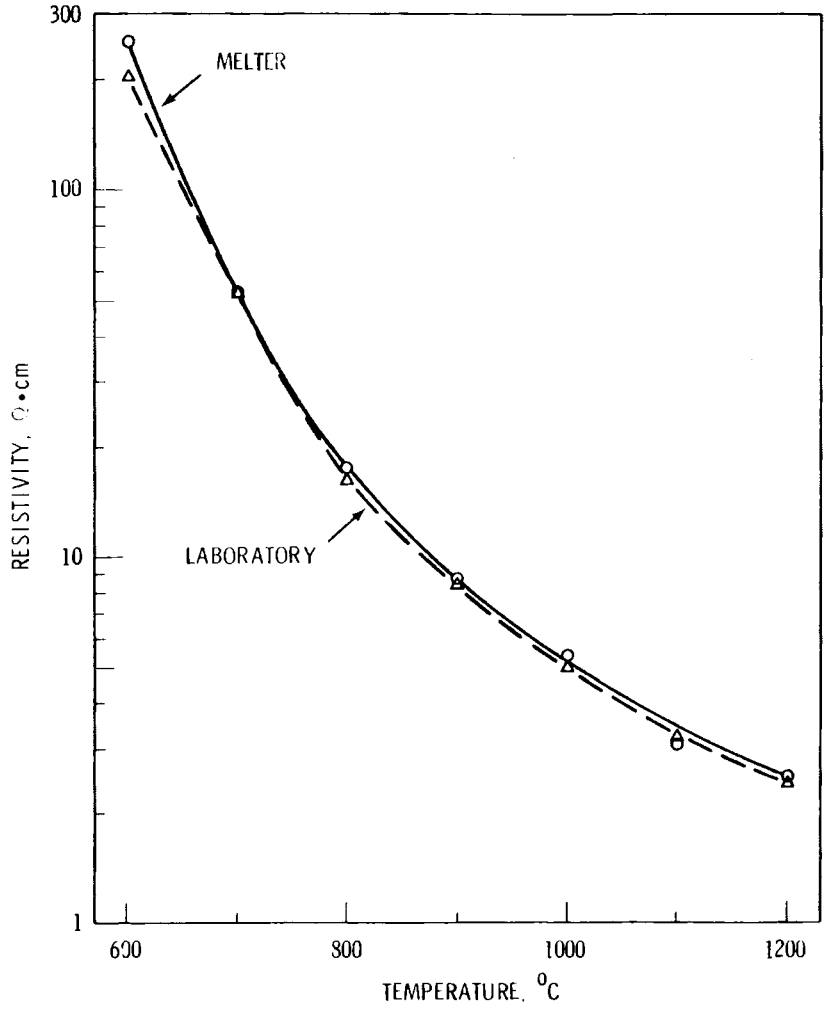

FIGURE 10. Electrical Resistivity Comparison of Melter- and Laboratory-Produced Glasses

TABLE 7. Comparative Leach Rates

Glass Composition	Percentage Weight Loss		
	Soxhlet (72-h, 99°C)	pH-4 (19-h, 23°C)	pH-9 (19-h, 23°C)
SRL TDS-411	6.4	25.0	0.1
72-68 (Commercial)	0.7	93.0	3.6
76-68 (Commercial)	5.8	0.17	0.2
Residual-liquid (melter-produced)	2.3	0.16	0.22

CONCLUSIONS

This series of tests demonstrates the technical feasibility of immobilizing Hanford residual-liquid waste in high-temperature borosilicate glass utilizing continuous-melting technology. The following conclusions can be drawn from the experience with this composition.

- The airlift draining technique employed by the HTCM does not increase glass porosity and provides good control of product glass flow.
- The residual-liquid waste can be effectively vitrified in engineering-scale equipment to produce a durable waste form exhibiting good leach resistance.
- High-temperature melting requires only minor changes in existing technology and does not significantly differ from low-temperature operation.
- The glass produced by the continuous melter demonstrates characteristics similar to the same glass formulation produced in the laboratory.
- Formation of fused, unreacted feed material caused by feed segregation can be eliminated by proper feed-mixing techniques.
- During processing, cesium volatility is comparable to low-melting borosilicate glass compositions.
- The maximum residual-liquid glass production rate for the HTCM was established at 18 kg/h--a melting flux rate of 160 kg/m^2-hour.

ACKNOWLEDGMENTS

The author gratefully acknowledges the assistance of L. E. Peterson in performing the residual-liquid glass tests and in the preparation of this report. Also deserving special thanks for their assistance in analyzing the many samples required for this report are H. H. Hollis and F. T. Hara.

REFERENCES

Buelt, J. L., et al. 1979. "A Review of Continuous Ceramic-Lined Melters and Associated Experience at PNL." PNL-SA-7590, Pacific Northwest Laboratory, Richland, Washington.

Chapman, C. C., et al. 1979. Vitrification of Hanford Wastes in a Joule-Heated Ceramic Melter and Evaluation of Resultant Canisterized Product. PNL-2904, Pacific Northwest Laboratory, Richland, Washington.

Gray, W. J. 1976. Volatility of a Zinc Borosilicate Glass Containing Simulated High-Level Radioactive Waste. BNWL-2111, Pacific Northwest Laboratory, Richland, Washington.

Kupfer, M. J. 1979. "Vitrification of Hanford Radioactive Defense Wastes." RHO-SA-89, Rockwell Hanford Operations, Richland, Washington.

Kupfer, M. J., and W. W. Schulz. 1973. Endothermic Process-Application to Immobilization of Hanford In-Tank Solidified Waste. ARH-2800, Atlantic Richfield Hanford Co., Richland, Washington.

McElroy, J. L., et al. 1980. Quarterly Progress Report - Research and Development Activities - High-Level Waste Immobilization Program: April Through June 1979. PNL-3050-2, Pacific Northwest Laboratory, Richland, Washington.

Ross, W. A., and J. E. Mendel. 1980. Annual Report on the Development and Characterization of Solidified Forms for High-Level Wastes: 1978. PNL-3060, Pacific Northwest Laboratory, Richland, Washington.

Rusin, J. M., et al. 1979. "Alternative Waste Forms--A Comparative Study." In Scientific Basis for Nuclear Waste Management, Vol. 2, ed. G. J. McCarthy, Plenum Press, New York, New York.

Schulz, W. W. 1980. "Removal of Radionuclides from Hanford Defense Waste Solutions." RHO-SA-51, Rockwell Hanford Operations, Richland, Washington.

DISTRIBUTION

No. of Copies

UNITED STATES

A. A. Churm
DOE Chicago Patent Division
9800 South Cass Avenue
Argonne, IL 60439

R. E. Cunningham
Deputy Director for Fuels and Materials
Nuclear Regulatory Commission
Silver Springs, MD 20910

Assistant Director for Radioactive Waste Management Branch
NRC Division of Materials and Fuel Cycle Facility Licensing
Washington, DC 20545

D. M. Rohrer
United States Nuclear Regulatory Commission
Washington, DC 20555

John Martin
United States Nuclear Regulatory Commission
Washington, DC 20555

W. G. Belter
DOE Division of Biomedical and Environmental Research
Earth Sciences Branch
Washington, DC 20545

W. A. Brobst
DOE Division of Environmental Control Technology
Washington, DC 20545

W. E. Mott
DOE Division of Environmental Control Technology
Washington, DC 20545

No. of Copies

R. B. Chitwood
DOE Division of Nuclear Power Development
Washington, DC 20545

T. C. Chee
DOE Office of Nuclear Waste Management
Washington, DC 20545

C. R. Cooley
DOE Office of Nuclear Waste Management
Washington, DC 20545

Sheldon Meyers
DOE Office of Nuclear Waste Management
Washington, DC 20545

R. G. Romatowski
DOE Office of Nuclear Waste Management
Washington, DC 20545

C. A. Heath
DOE Office of Nuclear Waste Management
Washington, DC 20545

G. Oertel
DOE Office of Nuclear Waste Management
Washington, DC 20545

A. F. Perge
DOE Office of Nuclear Waste Management
Washington, DC 20545

D. L. Vieth
DOE Office of Nuclear Waste Management
Washington, DC 20545

No. of Copies

R. D. Walton
DOE Office of Nuclear Waste Management
Washington, DC 20545

J. Neff, Program Manager
Department of Energy
Columbus Program Office
505 King Avenue
Columbus, OH 43201

J. B. Whitsett
DOE Idaho Operations Office
550 2nd Street
Idaho Falls, ID 83401

John Van Cleve
DOE Oak Ridge Operations Office
P.O. Box X
Oak Ridge, TN 37830

E. S. Goldberg
DOE Savannah River Operations Office
P.O. Box A
Aiken, SC 29801

27 DOE Technical Information Center

J. R. Berreth
Exxon Nuclear
Idaho Corporation
P. O. Box 2800
Idaho Falls, ID 83401

R. A. Brown
Exxon Nuclear
Idaho Corporation
P. O. Box 2800
Idaho Falls, ID 83401

Allied Chemical Corporation
(File Copy)
550 2nd Street
Idaho Falls, ID 83401

No. of Copies

M. D. McCormack
E.G. & G.Idaho, Inc.
P.O. Box 1625
Idaho Falls, ID 83401

W. C. Seymour
E.G. & G. Idaho, Inc.
P.O. Box 1625
Idaho Falls, ID 83401

R. A. Buckham
Allied-General Nuclear Service
P.O. Box 847
Barnwell, SC 29812

A. Williams
Allied-General Nuclear Service
P.O. Box 847
Barnwell, SC 29812

J. L. Jardine
Argonne National Laboratory
9700 South Cass Avenue
Argonne, IL 60439

M. M. Steindler/L. E. Trevorrow
Argonne National Laboratory
9700 South Cass Avenue
Argonne, IL 60439

J. M. Batch
Battelle Memorial Institute
505 King Ave.
Columbus, OH 43201

Wayne Carbiener
Battelle Memorial Institute
505 King Ave.
Columbus, OH 43201

J. D. Duguid
Battelle Memorial Institute
505 King Ave.
Columbus, OH 43201

No. of Copies

R. E. Heineman
Battelle Memorial Institute
505 King Ave.
Columbus, OH 43201

Battelle Memorial Institute
Office of Nuclear Waste Isolation
Attn: Beverly Rawles
505 King Avenue
Columbus, OH 43201

T. B. Hindman
E. I. duPont DeNemours and Company
Savannah River Laboratory
Aiken, SC 29801

J. Kircher
Office of Nuclear Waste Isolation
Battelle Memorial Institute
505 King Ave.
Columbus, OH 43201

Don Moak
Battelle Memorial Institute
505 King Ave.
Columbus, OH 43201

J. W. Voss
Office of Nuclear Waste Isolation
Battelle Memorial Institute
505 King Ave.
Columbus, OH 43201

Ken Yates
Battelle Memorial Institute
505 King Ave.
Columbus, OH 43201

Brookhaven National Laboratory
Reference Section
Information Division
Upton, NY 11973

No. of Copies

Paul W. Levy
Brookhaven National Laboratory
Upton, NY 11973

M. Steinberg
Brookhaven National Laboratory
Upton, NY 11973

Combustion Division
Combustion Engineering, Inc.
Windsor, CT 06095

B. Adams
Corning Glass Works
Technical Staffs Division
Corning, NY 14830

E. Vejvoda, Director
Chemical Operations
Rockwell International
Rocky Flats Plant
P.O. Box 464
Golden, CO 80401

J. L. Crandall
E. I. duPont DeNemours and Company
Savannah River Laboratory
Aiken, SC 29801

Jim Howel
E. I. dePont DeNemours and Company
Savannah River Laboratory
Aiken, SC 29801

H. L. Hull
E. I. duPont DeNemours and Company
Savannah River Laboratory
Aiken, SC 29801

R. G. Garvin
E. I. duPont DeNemours and Company
Savannah River Laboratory
Aiken, SC 29801

No. of
Copies

D. L. McIntosh
E. I. duPont DeNemours and Company
Savannah River Laboratory
Aiken, SC 29801

J. A. Kelley
E. I. duPont DeNemours and Company
Savannah River Laboratory
Aiken, SC 29801

M. D. Boersma
E. I. duPont DeNemours and Company
Savannah River Laboratory
Aiken, SC 29801

Robert Maher
E. I. duPont DeNemours and Company
Savannah River Laboratory
Aiken, SC 29801

S. Mirschak
E. I. duPont DeNemours and Company
Savannah River Laboratory
Aiken, SC 29801

J. K. Okeson
E. I. duPont DeNemours and Company
Savannah River Laboratory
Aiken, SC 29801

M. S. Plodinec
E. I. duPont DeNemours and Company
Savannah River Laboratory
Aiken, SC 29801

A. S. Jennings
E. I. duPont DeNemours and Company
Savannah River Laboratory
Aiken, SC 29801

No. of
Copies

Leon Meyers
E. I. duPont DeNemours and Company
Savannah River Laboratory
Aiken, SC 29801

H. Henning
Electric Power Research Institute
3412 Hillview Avenue
P.O. Box 10412
Palo Alto, CA 94301

Environmental Protection Agency
Technology Assessment Division (AW-559)
Office of Radiation Programs
Washington, DC 20460

R. G. Barnes
General Electric Company
175 Curtner Avenue (M/C 858)
San Jose, CA 95125

D. C. Fulmer
Savannah River Operations Office
P.O. Box A
Aiken, SC 29801

Los Alamos Scientific Laboratory (DOE)
P.O. Box 1663
Los Alamos, NM 87544

John Pomeroy
Technical Secretary
National Academy of Sciences
Committee of Radioactive Waste Management
National Research Council
2101 Constitution Avenue
Washington, DC 20418

J. P Duckworth
Plant Manager
Nuclear Fuel Services, Inc.
P.O. Box 124
West Valley, NY 14171

No. of
Copies

Oak Ridge National Laboratory
(DOE)
Central Research Library
Document Reference Section
P.O. Box X
Oak Ridge, TN 37830

W. Weart
Sandia Laboratories
Albuquerque, NM 87107

J. O. Blomeke
Union Carbide Corporation (ORNL)
Chemical Technology Division
P.O. Box Y
Oak Ridge, TN 37830

R. E. Blanco
Union Carbide Corporation (ORNL)
Chemical Technology Division
P.O. Box Y
Oak Ridge, TN 37830

E. Newman
Union Carbide Corporation (ORNL)
Chemical Technology Division
P.O. Box Y
Oak Ridge, TN 37830

A. L. Lotts
Union Carbide Corporation (ORNL)
Chemical Technology Division
P.O. Box Y
Oak Ridge, TN 37830

W. J. Lackey
Union Carbide Corporation (ORNL)
Chemical Technology Division
P.O. Box Y
Oak Ridge, TN 37830

T. Lindemer
Union Carbide Corporation (ORNL)
Chemical Technology Division
P.O. Box Y
Oak Ridge, TN 37830

No. of
Copies

D. E. Ferguson
Union Carbide Corporation (ORNL)
Chemical Technology Division
P.O. Box Y
Oak Ridge, TN 37830

H. W. Godbee
Union Carbide Corporation (ORNL)
Chemical Technology Division
P.O. Box Y
Oak Ridge, TN 37830

R. G. Post
College of Engineering
University of Arizona
Tucson, AZ 85721

S. E. Logan
Los Alamos Technical
Associates, Inc.
P.O. Box 410
Los Alamos, NM 87544

FOREIGN

2 International Atomic Energy
Agency
Wagram erstrasse 5
P.O. Box 100
A-1400, Vienna, AUSTRIA

Rene Amavis
EURATOM
Health Physics Division
29, Rue Aldringer
Luxembourg, BELGIUM

G. G. Strathdee
Atomic Energy of Canada, Ltd.
W.N.R.E. Pinawa, Manitoba
ROE 1LO
CANADA

No. of Copies

M. Tomlinson
Director of Chemistry and Materials Science Division
Atomic Energy of Canada Ltd.
Whiteshell Nuclear Research Establishment
Pinawa, Manitoba, CANADA

K. D. B. Johnson
Atomic Energy Research Establishment,
Harwell, Didcot,
Berks, ENGLAND

J. A. C. Marples
Atomic Energy Research Establishment
Harwell, Didcot,
Berks, ENGLAND

D. W. Clelland
United Kingdom Atomic Energy Authority
Risley, ENGLAND

B. Morris
Atomic Energy Research Establishment,
Harwell, Didcot,
Berks, ENGLAND

P. J. Regnaut
Centre d'Etudes Nucleaires de Fontenay-aux Roses
Boite Postale 6
92 - Fontenay-aux Roses
FRANCE

Dr. P. G. Alfredson
Chief, Chemical Technology Division
Australian Atomic Energy Commission
Research Establishment
Lucas Heights, New South Wales, 2232

No. of Copies

Library
Studsvik Energiteknik AB
S-611 01Nykoping
SWEDEN

Bundesministerium fur Forschung und Technologie
Stressemannstrasse 2
5300 Bonn
WEST GERMANY

Center for Atomic Energy Documentation (ZAED)
Attn: Dr. Mrs. Bell
P. O. Box 3640
7500 Karlsruhe
WEST GERMANY

Hans W. Levi
Hahn-Meitner Institut
1 Berlin 39
Glienickerstr. 100
WEST GERMANY

E. R. Merz
Institut fur Chemische Technologie
Kernforschungsanloge Julich GmbH
D517 Julich
Postfach 365
Federal Republic
WEST GERMANY

R. Bonniaud
Center de Marcoule
B.P. 170
30200 Baguols-Sur-Ceze
FRANCE

C. Sombret
Centre de Marcoule
B.P. 170
30200 Baguols-Sur-Ceze
FRANCE

No. of
Copies

F. Laude
Centre de Marcoule
B.P. 170
30200 Baguols-Sur-Ceze
FRANCE

H. Krause
Kernforschungszentrum Karlsruhe
GmbH (KfK)
Postfach 3640
D7500 Karlsruhe
WEST GERMANY

R. V. Amalraj
C.W.M.F. Project
P.O. Kalpakkam
Chingleput Dist.
Tamil Nadu, INDIA

N. S. Sunder Rajan
Bhabha Atomic Research Centre
Goverment of India
Hall No. 5
Trombay
Bombay 8S
INDIA

Dr. Piero Risoluti,
AGIP NUCLEARE
c/o COMB Casaccia
C.P. 2400
Rome
ITALY

F. Gera
CHEN
CSN Casaccia L.I.S.
C.P. 2400, 00100
Rome
ITALY

No. of
Copies

S. Tashiro
Japan Atomic Energy Research
Institute
Environmental Safety Research
Laboratory
1-1-13, Shibashi
Minatopku, Tokyo
JAPAN

ONSITE

4 DOE Richland Operations Office

P. A. Craig
H. E. Ransom
M. W. Shupe
M. J. Zamorski

30 Rockwell Hanford Operations

H. Babad
R. A. Deju
R. J. Gimera
D. R. Gustavson
D. R. Harlow
B. A. Higley (10)
E. J. Kosiancic
M. J. Kupfer (5)
C. M. Manry
R. C. Raal
I. E. Reep
J. H. Roecker
W. W. Schulz
M. J. Smith
R. A. Wetrous
D. D. Wodrich
File copy

3 Exxon Nuclear Company

S. J. Beard

Joint Center for Graduate
Study

J. Cooper

No. of
Copies

2 United Nuclear Industries, Inc.

T. E. Dabrowski
A. E. Engler

Westinghouse Hanford Company

A. G. Blasewitz

59 Pacific Northwest Laboratory

S. M. Barnes (20)
W. J. Bjorklund
H. T. Blair
W. F. Bonner
R. A. Brouns
J. L. Buelt
R. D. Dierks
M. S. Hanson
A. J. Haverfield
M. H. Henry (3)
O. F. Hill
L. K. Holton
J. H. Jarrett
D. E. Knowlton
C. A. Knox
W. L. Kuhn
D. E. Larson
J. L. McElroy
G. B. Mellinger
J. E. Mendel
F. A. Miller
R. E. Nightingale
K. H. Oma
A. M. Platt
D. L. Prezbindowski (2)
J. M. Rusin
D. H. Siemens
S. C. Slate
C. L. Timmerman
R. T. Treat
R. E. Westerman
Technical Information (5)
Publishing Coordination (2)